RNA

Exon junction complex modulates m^{6}A distribution

*N*6-methyladenosine (m^{6}A) is the most prevalent base modification in the mammalian transcriptome and is reported to have roles in many cellular processes, including RNA splicing and stability. It is deposited at DRACH motifs (D = A/G/U R = A/G, H = A/C/U) by the METTL3–METTL14 methyltransferase complex, although only a fraction of these motifs is modified in cellular RNA. Moreover, m^{6}A is deposited unevenly along mRNAs, with highest levels found in 3′ untranslated regions (UTRs) and within unusually long internal exons, but the mechanism underlying this non-uniform modification pattern has been unclear. Now, two studies demonstrate that the exon junction complex (EJC) helps to shape this characteristic distribution by excluding m^{6}A from exon junctions.

In the first study, Yang et al. showed that m^{6}A is more sparsely and uniformly distributed in nascent mRNA than mature mRNA, suggesting that the distinctive m^{6}A distribution develops dynamically during mRNA processing. Thus, they next investigated the known link between m^{6}A demethylases (ALKBH5 and FTO) and splicing by performing immunoprecipitations with ALKBH5 and FTO to identify interacting splicing-related proteins. The protein that interacted most strongly with ALKBH5 was EIF4A3, the RNA-binding component of the EJC, which is deposited 24 nucleotides upstream of exon junctions during splicing and remains bound after mRNAs are transported to the cytoplasm. The effects of these proteins on m^{6}A in mature mRNAs were tested by small interfering RNA (siRNA)-based knock-down analysis. Whereas depletion of ALKBH5 had minimal effects on global m^{6}A levels, knock down of EIF4A3 resulted in a dramatic increase in m^{6}A. Regions with increased m^{6}A (short internal exons and regions close to splice junctions of long internal exons) were consistent with regions at which EJC is known to assemble. These results indicate that EIF4A3 restricts m^{6}A levels at exon junctions, but not by promoting demethylation.

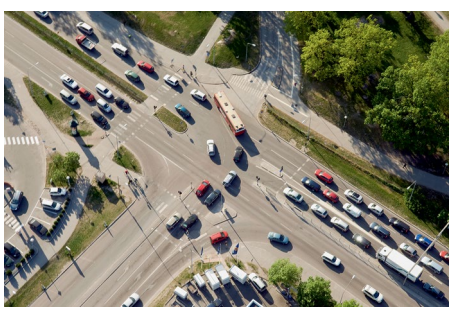

To determine if EIF4A3 might instead interfere with deposition of m^{6}A, the effect of siRNA-mediated depletion of EIF4A3 on transcriptome-wide METTL3 occupancy was assessed. Not only did METTL3 occupancy increase with EIF4A3 depletion, but regions of increased occupancy highly correlated with regions that had higher m^{6}A levels in EIF4A3-depleted cells. Analysis of reporter constructs confirmed that the effect of EIF4A3 on METTL3 occupancy and m^{6}A levels was dependent on splicing, and that tethering of EIF4A3 to exon junctions was sufficient to suppress binding of METTL3 and m^{6}A deposition. These observations are consistent with a model whereby the assembly of EJC at exon junctions during splicing restricts the accessibility of these regions to METTL3 and deposition of m^{6}A, leading to comparatively higher levels of m^{6}A at more accessible, EJC-depleted regions such as the 3′UTR.

Uzonyi et al. reached similar conclusions but by a different route. They began by showing that an intact DRACH motif was both necessary and sufficient for m^{6}A deposition, with m^{6}A levels reflecting the number of motifs present — except in the proximity of introns, which seemed to inhibit modification of nearby motifs. They generated a computational model (m^{6}Apred-1) to predict m^{6}A distribution based on the modification of all eligible DRACH motifs (the seven most prevalent consensus sequences) within the mRNA; this model better predicted m^{6}A patterns for genes lacking introns than those containing them, further supporting the notion that introns influence m^{6}A distribution. Analysis of multiple publicly available single-nucleotide resolution transcriptome-wide m^{6}A datasets indicated that m^{6}A was depleted within ~200 nucleotides of exon junctions. The dependence of these m^{6}A 'exclusion zones' on proximity to an exon–intron border was confirmed experimentally and a fixed size exclusion zone parameter (within 100 nucleotides of an exon–intron junction) was incorporated into an updated computational model (m^{6}Apred-2). This new model more accurately captured m^{6}A distribution in exon-containing genes than did m^{6}Apred-1, confirming the importance of exon–intron architecture in shaping m^{6}A distribution.

Exon–intron architecture — specifically exon density — has been reported to be strongly correlated with RNA stability, and RNA stability to be inversely correlated with m^{6}A levels. Analysis of both existing and newly generated data by Uzonyi et al. confirmed these relationships but also showed that exon density and m^{6}A levels were inversely correlated. Notably, reducing m^{6}A levels via METTL3 depletion abrogated the correlation between exon density and RNA stability, indicating that m^{6}A is the mechanistic link between exon density and RNA stability.

Finally, given that EJC binds to exon junctions (that is, within m^{6}A exclusion zones), the authors investigated its role in modulating m^{6}A distribution. Degron-mediated depletion of Y14, a core EJC component, resulted in an increase of m^{6}A within, but not outside of, exclusion zones. Additionally, m^{6}Apred-2 became less predictive of m^{6}A distribution as cells were depleted of Y14 whereas m^{6}Apred-1 became more so. These data indicate that EJC is responsible for establishing m^{6}A exclusion zones at exon boundaries. In conclusion, Uzonyi et al. propose that m^{6}A distribution is dependent on sequence motifs and exon-intron architecture, whereby DRACH motifs are m^{6}A modified by default unless they are in proximity to an EJC-bound splice junction.

Now that the mechanism underlying m^{6}A distribution has been established, it will be interesting to investigate whether it has functional significance beyond the link to RNA stability established here.

Dorothy Clyde

Original articles: Yang, X. et al. Exon junction complex shapes the m6A epitranscriptome. *Nat. Commun.* **13**, 7904 (2022); Uzonyi, A. et al. Exclusion of m6A from splice-site proximal regions by the exon junction complex dictates m6A topologies and mRNA stability. *Mol. Cell* https://doi.org/10.1016/j.molcel.2022.12.026 (2023)